Front. Electr. Electron. Eng. China 2009, 4(3): 342–347
DOI 10.1007/s11460-009-0050-x

RESEARCH ARTICLE

Yuhui HE, Yuning ZHAO, Chun FAN, Xiaoyan LIU, Ruqi HAN

Simulation of inhomogeneous strain in Ge-Si core-shell nanowires

© Higher Education Press and Springer-Verlag 2009

Abstract This paper studies the elastic deformation field in lattice-mismatched Ge-Si core-shell nanowires (NWs). Infinite wires with a cylindrical cross section under the assumption of translational symmetry are considered. The strain distributions are found by minimizing the elastic energy per unit cell using finite element method. This paper finds that the trace of the strain is discontinuous with a simple, almost piecewise variation between core and shell, whereas the individual components of the strain can exhibit complex variations. The simulation results are prerequisite of strained band structure calculation, and pave a way for further investigation of strain effect on the related transport property simulation.

Keywords core-shell nanowire, strain, continuum elasticity

1 Introduction

Recently, by introducing heterostructures along the radial orientation of nanowires (NWs), more complex core-shell nanowire structures have been prepared, with both IV [1,2] and III-V [3–5] semiconductor materials. The epitaxial shell removes the surface states from the core thereby further improving the electrical properties. Besides, the lattice mismatches between the core and shell induces pseudomorphic strain in the core and provides more flexibility in band structure modulations.

On device application, Ge-Si core-shell nanowire field effect transistors (FETs) have been realized experimentally and demonstrated excellent electrical properties [6,7]. To drive future experiments, a computational study of this novel transistor structure is imperative. In this respect, an appropriate modeling of the inhomogeneous strain induced by the core-shell (C-S) lattice mismatch in Ge-Si C-S NW is essential [8]. Only with strain distribution obtained can the strain effect on NW band structures and on NW FET performance be evaluated.

In this article, we discuss and calculate the strain field in lattice-mismatched Ge-Si core-shell nanowires. We find rich behavior of the individual strain components, whereas their combination, the trace of the strain tensor (the volumetric strain), shows much less variation.

2 Theory and method

In this work, we calculate the elastic deformation field in lattice-mismatched Ge-Si core-shell nanowires (see Fig. 1 for schematics). As an approximation, we take the nanowires as infinite with translational symmetry along the growth direction. We argue below (based on Saint-Venant's principle) that our description of the infinite wires is also relevant to long finite wires. For simplicity, we neglect exterior forces acting on the surface or bulk parts of the wires, i.e., we consider free nanowires. Furthermore, we consider only wires grown in the [1 1 0]-direction in this work. For convenience, we define a primed coordinate system with respect to the growth direction, having basis vectors,

$$\hat{x} = \frac{1}{2}\begin{bmatrix} 1 \\ -1 \\ -\sqrt{2} \end{bmatrix}, \tag{1a}$$

$$\hat{y} = \frac{1}{2}\begin{bmatrix} -1 \\ 1 \\ -\sqrt{2} \end{bmatrix}, \tag{1b}$$

Received January 12, 2009; accepted March 16, 2009

Yuhui HE, Yuning ZHAO, Xiaoyan LIU, Ruqi HAN (✉)
Institute of Microelectronics, Peking University, Beijing 100871, China
E-mail: hanrq@ime.pku.edu.cn

Chun FAN
Computer Center of Peking University, Beijing 100871, China

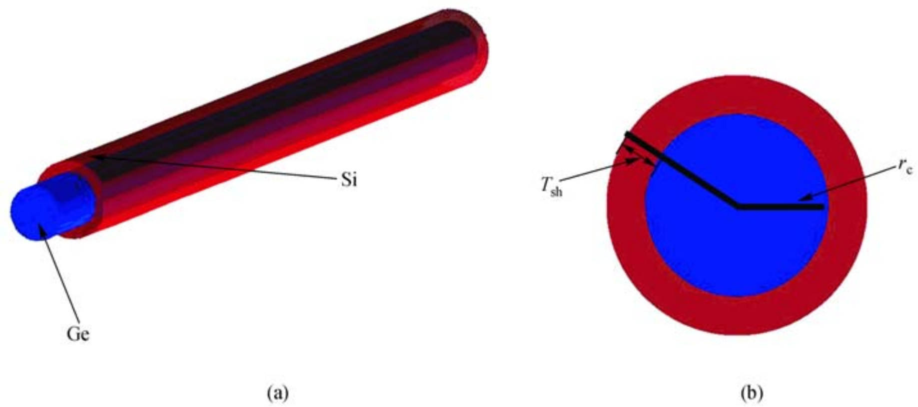

Fig. 1 Schematic view of Ge-Si core-shell nanowires. (a) Side view of Ge-Si core-shell nanowire; (b) top view of Ge-Si core-shell nanowire

$$\hat{z} = \frac{1}{\sqrt{2}}\begin{bmatrix} 1 \\ 1 \\ 0 \end{bmatrix}. \tag{1c}$$

Consider, for example, a core-shell nanowire with undeformed core and shell axial lengths of L_c and L_s and lattice constants of $a^{(c)}$ and $a^{(s)}$. To allow for pseudomorphic matching, we shall assume that both core and shell have the same number N of unit cells in the axial direction and, thus, L_c must necessarily differ from L_s. We can write

$$\frac{L_c}{a^{(c)}} = \frac{L_s}{a^{(s)}} = CN, \tag{2}$$

where C is some constant of proportionality.

To match the lattice of the shell to the core we introduce the pseudomorphic initial strain field $\varepsilon^{(0)}$ in the shell. This choice of the pseudomorphic strain field initially scales all shell lattice vectors to have the same length as in the core [9],

$$(1+\varepsilon^{(0)})a^{(s)} = a^{(c)}. \tag{3}$$

In this approximation, the only non-zero strains are ε'_{xx}, ε'_{yy} and ε'_{xy}, whereas $\varepsilon'_{zx} = \varepsilon'_{zy} = 0$ (planar sections remain flat) and ε'_{zz} along the nanowire axial direction.

For the Ge-Si core-shell nanowires we consider in this work, ε'_{zz} is not known a priori, but we expect it to be present due to the lattice mismatch. Therefore, we introduce an ε'_{zz} for each sub-domain of a nanowire and consider these strains as variables. In the simple case of a core-shell structure with two sub-domains (the core and the shell), the matching effectively reduces the two axial strains $\varepsilon^{(c)}_{zz}$ and $\varepsilon^{(s)}_{zz}$ to a single variable a_z:

$$\varepsilon^{(i)}_{zz} = \frac{a_z}{a^{(i)}_z} - 1, \quad i = \mathrm{c,s}. \tag{4}$$

Generally, the potential elastic energy is written in $\boldsymbol{e}_x$=[1 0 0], $\boldsymbol{e}_y$=[0 1 0] and $\boldsymbol{e}_z$=[0 0 1] coordinate [10,11],

$$U = \frac{1}{2}\iiint \mathrm{d}V u(\boldsymbol{r})$$
$$= \iiint \mathrm{d}V \boldsymbol{\varepsilon}^{\mathrm{T}}(\boldsymbol{r}) \begin{bmatrix} C_{11} & C_{12} & C_{12} & & & \\ C_{12} & C_{11} & C_{12} & & & \\ C_{12} & C_{12} & C_{11} & & & \\ & & & C_{44} & 0 & 0 \\ & & & 0 & C_{44} & 0 \\ & & & 0 & 0 & C_{44} \end{bmatrix}, \tag{5}$$

where $\boldsymbol{\varepsilon}^{\mathrm{T}} = [\varepsilon_{xx}, \varepsilon_{yy}, \varepsilon_{zz}, \varepsilon_{yz}, \varepsilon_{xz}, \varepsilon_{xy}]$ is the strain tensor, C_{11}, C_{12} and C_{44} are material elastic modulus.

We transform it to the primed coordinate of nanowires:

$$U = \iiint \mathrm{d}V \frac{1}{2}\Big[D_1({\varepsilon'_{xx}}^2 + {\varepsilon'_{yy}}^2) + D_2{\varepsilon'_{xy}}^2 + D_3{\varepsilon'_{zz}}^2 + D_4\varepsilon'_{xx}\varepsilon'_{yy} + (\varepsilon'_{xx} + \varepsilon'_{yy})(D_5\varepsilon'_{zz} + D_6\varepsilon'_{xy})\Big], \tag{6}$$

with the constants

$$D_1 = (6C_{11} + 10C_{12} + 5C_{44})/16,$$
$$D_2 = (6C_{11} - 6C_{12} + C_{44})/4,$$
$$D_3 = (2C_{11} + 2C_{12} + C_{44})/4,$$
$$D_4 = (6C_{11} + 10C_{12} - 3C_{44})/8,$$
$$D_5 = (2C_{11} + 6C_{12} - C_{44})/4,$$
$$D_6 = (2C_{11} - 2C_{12} - C_{44})/4,$$

ε'_{ij} is strain tensor in the primed coordinate. From now on, we write it as ε_{ij} for simplicity since we work in the primed coordinate. For core-shell nanowire heterostructures, the elastic energy consists of two parts, that in the core and in the shell [12]:

$$U = U_{\mathrm{c}} + U_{\mathrm{s}}, \tag{7}$$

with expressions as follows:

$$U_{\mathrm{c(s)}} = \int \mathrm{d}S_{\mathrm{c(s)}} \frac{1}{2} \left[D_1^{\mathrm{c(s)}} (\Delta\varepsilon_{xx}^2 + \Delta\varepsilon_{yy}^2) + D_2^{\mathrm{c(s)}} \varepsilon_{xy}^2 + D_3^{\mathrm{c(s)}} \left(\frac{a_z - a_z^{\mathrm{c(s)}}}{a_z^{\mathrm{c}}} \right)^2 + D_4^{\mathrm{c(s)}} \Delta\varepsilon_{xx} \Delta\varepsilon_{yy} + (\Delta\varepsilon_{xx} + \Delta\varepsilon_{yy}) \left(D_5^{\mathrm{c(s)}} \frac{a_z - a_z^{\mathrm{c(s)}}}{a_z^{\mathrm{c}}} + D_6^{\mathrm{c(s)}} \varepsilon_{xy} \right) \right]. \tag{8}$$

Here $\Delta\varepsilon_{ii} = \varepsilon_{ii} - \varepsilon_{ii}^{\mathrm{c(s)}}$. For Ge core, $\varepsilon_{ii}^{\mathrm{c}} = 0$; while for Si shell $\varepsilon^{\mathrm{s}} = (a_i^{\mathrm{s}} - a_i^{\mathrm{c}})/a_i^{\mathrm{c}}$. Mathematically, strain energy U is now an integral functional $U[\varepsilon_{xx}(\boldsymbol{r}),\varepsilon_{yy}(\boldsymbol{r})\ \varepsilon_{xy}(\boldsymbol{r}),a_z]$ [13,14].

The potential energy allows us to find the deformation field by a variational principle:

$$\frac{\delta U}{\delta \varepsilon_{ij}} = 0, \quad \frac{\partial U}{\partial a_z} = 0. \tag{9}$$

In the numerical simulations, we have used linear finite element method (FEM) [15], and all the material parameters were taken from Ref. [16].

3 Numerical results

First, we demonstrate the strain energy density distribution $u(\boldsymbol{r})$ in Ge-Si C-S NW cross-sections in Fig. 2. Here the Ge core radius is 7 nm, and Si shell thickness varies from 1 nm (Fig. 2(a)), to 2 nm (Fig. 2(b)) and to 3 nm (Fig. 2(c)). It is seen that $u(\boldsymbol{r})$ is quite homogeneous in the core compared with that in the shell. We attribute this to the eggshell principle in engineering: as long as the shell is round and perfect, the egg is able to disperse the stress over the whole shell homogeneously. Furthermore, $u(\boldsymbol{r})$ in the shell has a cubic symmetry due to the equivalence between lattice orientations $\boldsymbol{e}_x$ and $\boldsymbol{e}_y$.

Now we demonstrate the strain tensor distribution ε_{xx}, ε_{yy}, and ε_{xy} in Ge-Si C-S NW cross-sections in Fig. 3. Here the Ge core radius r_{c} is 6 nm, and Si shell thickness T_{sh} is 2 nm. We find that along y-oriented interface between Ge core and Si shell, $\varepsilon_{yy} < 0$ in the core side while $\varepsilon_{yy} > 0$ in the shell side. The former indicates a compressive strain while the latter means a tensile strain. It is as expected since Ge has a larger lattice constant than Si does. Similar explanations apply to ε_{xx}.

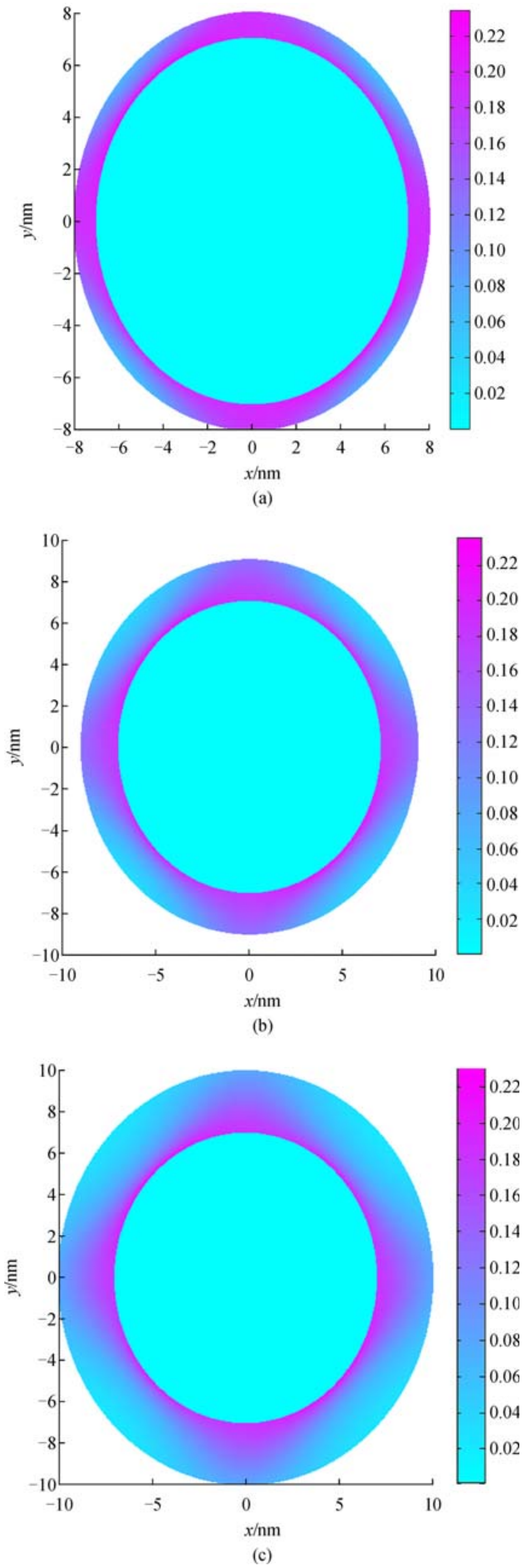

Fig. 2 Distribution of strain energy in NW cross-section. (a) Ge core radius $r_{\mathrm{c}} = 7$ nm and Si shell thickness $T_{\mathrm{sh}} = 1$ nm; (b) $r_{\mathrm{c}} = 7$ nm and $T_{\mathrm{sh}} = 2$ nm; (c) $r_{\mathrm{c}} = 7$ nm and $T_{\mathrm{sh}} = 3$ nm

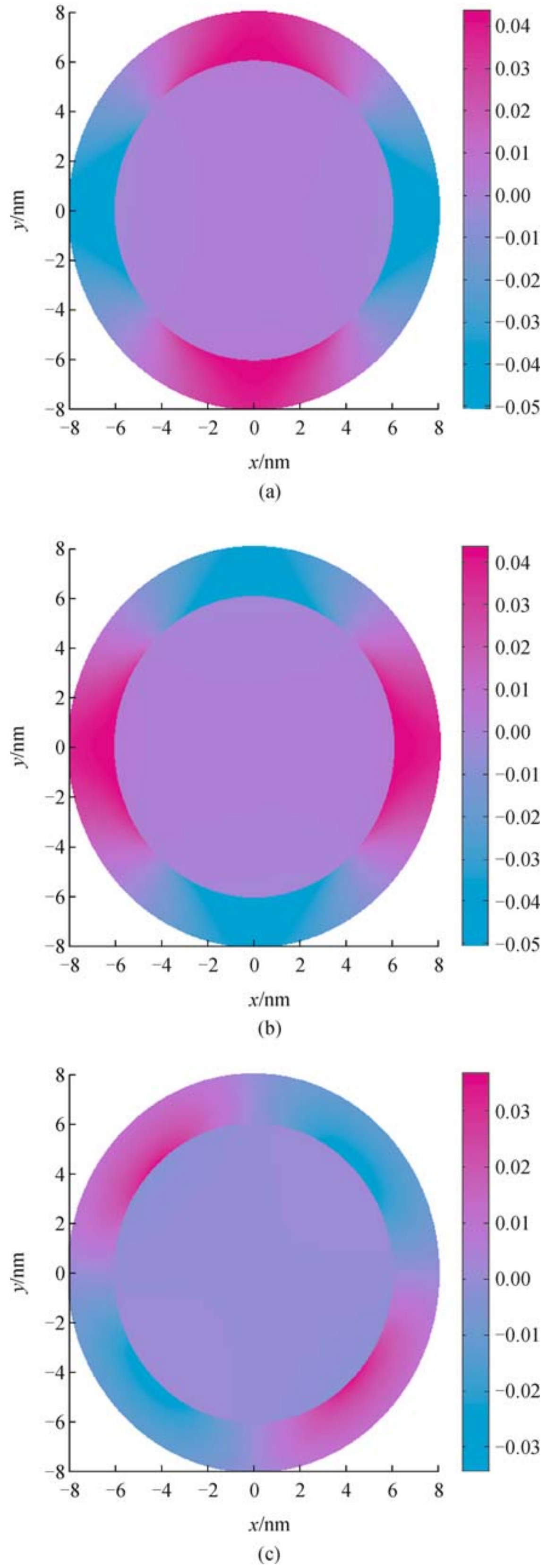

Fig. 3 Distribution of strain tensor components $\varepsilon_{ij}(\boldsymbol{r})$ in NW cross-section, with $r_c = 6$ nm and $T_{sh} = 2$ nm. (a) $\varepsilon_{xx}(\boldsymbol{r})$; (b) $\varepsilon_{yy}(\boldsymbol{r})$; (c) $\varepsilon_{xy}(\boldsymbol{r})$

Last but not least, we plot the NW axial strain tensor ε_{zz} in Ge core and Si shell as a function of shell thickness in Fig. 4. We observe that when Si shell grows thicker, ε_{zz}^{c} increases while ε_{zz}^{s} decreases. At the extreme thickness of Si shell, ε_{zz}^{c} approaches the saturation value

$$\frac{a_{Si}}{a_{Ge}} - 1 = -3.81\%,$$

while ε_{zz}^{s} approaches 0. The physical mechanism is that lattice distance of Ge core has been compressed so much that it approaches that of Si shell, since Si shell volume has overwhelmed that of Ge core.

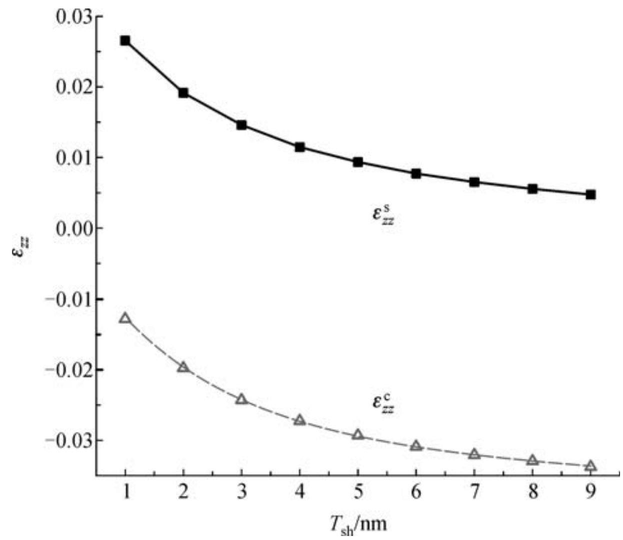

Fig. 4 NW axial strain ε_{zz} in Ge core (ε_{zz}^{c}: dash-triangle line) and in Si shell (ε_{zz}^{s}: solid-square line) versus Si shell thickness T_{sh}. Here $r_c = 6$ nm

We further plot the strain energy and strain tensor distribution in a Ge-Si-Ge core-multishell NW cross-section in Fig. 5. The multishell structure provides further flexibility of the strain magnitude tuning in NW. The radius of the core, the thickness of inner shell and outer shell are taken to be $r_c = 6$ nm, $T_{sh} = 3$ nm and $T_{sh}^{out} = 2$ nm. Similar to the case of single-shell, strain energy and strain tensor are small and homogeneous in the core NW. Besides, since the lattice constant of the inner shell is larger than that of its surroundings, the horizontal parts of the exterior shell near the interface undergoes considerable stretching as in the single shell case, see ε_{xx}^{s} in Fig. 3(a).

4 Conclusions

This paper presents a theoretical study of the strain field in Ge-Si lattice-mismatched core-shell nanowires, and derives a functional for the elastic energy. The strain distribution is found by minimization of the energy

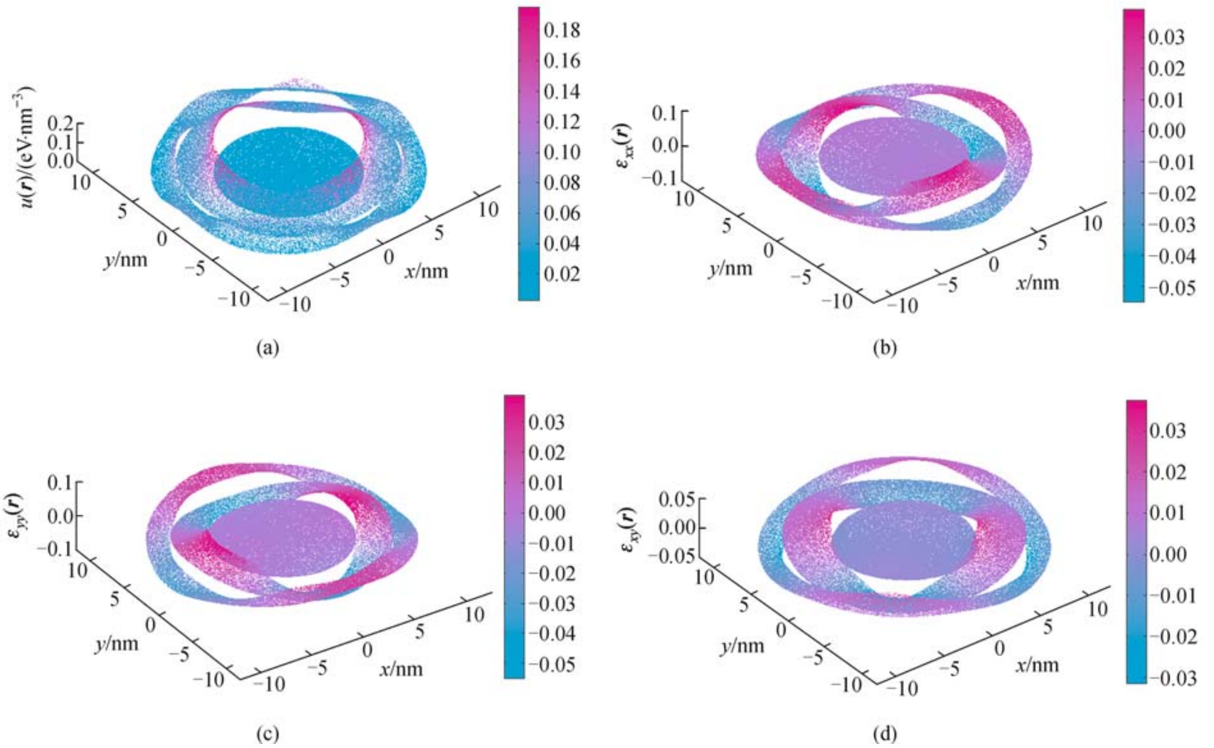

Fig. 5 Distribution of strain energy $u(\boldsymbol{r})$ and strain tensor components $\varepsilon_{ij}(\boldsymbol{r})$ in cross-section of Ge-Si-Ge core-multishell NW, with Ge core radius $r_c = 6$ nm, Si shell thickness $T_{sh} = 3$ nm, and outer Ge shell thickness $T_{sh}^{out} = 2$ nm. (a) Strain energy; (b) $\varepsilon_{xx}(\boldsymbol{r})$; (c) $\varepsilon_{yy}(\boldsymbol{r})$; (d) $\varepsilon_{xy}(\boldsymbol{r})$

functional using finite element method. We find a large compression appearing in the core region, which will influence carriers via the deformation potential. Our work provides physical modeling and understanding of the strain distribution in C-S NW, and the obtained quantitative results serve as the bases of strained valence band calculation and transport simulation in further work.

References

1. Lauhon L J, Gudiksen M S, Wang D, Lieber C M. Epitaxial core-shell and core-multishell nanowire heterostructures. Nature, 2002, 420(6911): 57–61
2. Lu W, Xiang J, Timko B P, Wu Y, Lieber C M. One-dimensional hole gas in germanium/silicon nanowire heterostructures. Proceedings of the National Academy of Sciences of the United States of America, 2005, 102(29): 10046–10051
3. Lin H M, Chen Y L, Yang J, Liu Y C, Yin K M, Kai J J, Chen F R, Chen L C, Chen Y F, Chen C C. Synthesis and characterization of core-shell GaP@GaN and GaN@GaP nanowires. Nano Letters, 2003, 3(4): 537–541
4. Tateno K, Gotoh H, Watanabe Y. GaAs/AlGaAs nanowires capped with AlGaAs layers on GaAs(311)B substrates. Applied Physics Letters, 2004, 85(10): 1808–1810
5. Sköld N, Karlsson L S, Larsson M W, Pistol M E, Seifert W, Tragardh J, Samuelson L. Growth and optical properties of strained GaAs-$Ga_xIn_{1-x}P$ core-shell nanowires. Nano Letters, 2005, 5(10): 1943–1947
6. Xiang J, Lu W, Hu Y, Wu Y, Yan H, Lieber C M. Ge/Si nanowire heterostructures as high-performance field-effect transistors. Nature, 2006, 441(7092): 489–493
7. Liang G, Xiang J, Kharche N, Klimeck G, Lieber C M, Lundstrom M. Performance analysis of a Ge/Si core/shell nanowire field-effect transistor. Nano Letters, 2007, 7(3): 642–646
8. Liu X W, Hu J, Pan B C. The composition-dependent mechanical properties of Ge/Si core-shell nanowires. Physica E: Low-dimensional Systems and Nanostructures, 2008, 40(10): 3042–3048
9. De Caro L, Tapfer L. Elastic lattice deformation of semiconductor heterostructures grown on arbitrarily oriented substrate surfaces. Physical Review B, 1993, 48(4): 2298–2303
10. Landau L, Lifshitz E. Theory of Elasticity. New York: Pergamon, 1959
11. Pryor C, Kim J, Wang L W, Williamson A J, Zunger A. Comparison of two methods for describing the strain profiles in quantum dots. Journal of Applied Physics, 1998, 83(5): 2548–2550
12. Jogai B. Three-dimensional strain field calculations in coupled InAs/GaAs quantum dots. Journal of Applied Physics, 2000, 88(9): 5050–5055
13. Cleland A N. Foundations of Nanomechanics. Berlin: Springer, 2003
14. Søndergaard N, He Y H, Fan C, Han R Q, Guhr T, Xu H Q. Strain

distributions in lattice mismatched semiconductor core-shell nanowires. Journal of Vacuum Science and Technology B, 2009, 27(2): 827–830

15. Zienkiewicz O C, Taylor R L. The Finite Element Method. Maidenhead: McGraw-Hill, 1994
16. Vurgaftman I, Meyer J R, Ram-Mohan L R. Band parameters for III-V compound semiconductors and their alloys. Journal of Applied Physics, 2001, 89(11): 5815–5875